AJCHE 2011, Vol. 11, No. 2, 1 – 7

Modeling of the Drying Kinetics of Slurry Droplet in Spray Drying

Boris Golman
School of Chemical Engineering, Institute of Engineering, Suranaree University of Technology, 111 University Avenue, Muang District, Nakhon Ratchasima, 30000, Thailand.
E-mail: golman@sut.ac.th

The detail analysis of the heat and mass transfer between the droplet containing suspended solids and the drying gas was carried out numerically. The temperature and moisture distributions within the slurry droplet were calculated during the first and second drying phases. The parametric study revealed that the droplet drying time decreases with increasing the drying gas temperature and decreasing the droplet diameter.

Keyword: Spray Drying, Slurry, Drying Kinetics, Heat Transfer, Mass Transfer, Modeling

SELECTION

- Numerical analysis of the heat and mass transfer between the droplet containing suspended solids and the drying gas
- Calculation of temperature and moisture distributions within the slurry droplet during the first and second drying phases.

INTRODUCTION

The agglomerates of fine particles produced by spray drying have found expanding applications in chemical (Okuyama et al., 2006), pharmaceutical (Soottitantawat et al., 2005), food (Gharsallaoui et al., 2007) and agriculture (Elek et al., 2010) industries as high-value functional materials.

Spray drying is a complex process involving simultaneous heat, mass and momentum transfer between the drying gas and droplets as well as possible formation of solid phase in the droplet during drying (Masters, 1985).

The kinetics of drying process depends on the temperature and moisture distributions within the slurry droplet. The drying process of a slurry droplet can be divided into two stages according to the droplet morphology (Mezhericher et al., 2010). The droplet shrinks throughout the first drying phase due to liquid evaporation until the dry solid crust is formed around the wet core at the beginning of the second drying phase. Then, the wet particle of constant outer diameter is dried till attainment of final moisture content.

Theoretical models of drying of a slurry droplet are mainly based on the droplet average temperature and moisture content or the temperature distribution within the droplet is considered only in the crust region during the second drying phase (Mezhericher et al., 2010).

Therefore, there is a need to develop a detail model of drying kinetics capable of describing the temperature and moisture distributions within the slurry droplet during the first and second drying phases.

THEORY

First phase of drying

During the first phase of drying, water evaporates from the slurry droplet at constant rate as a result of heat transfer from surrounding gas by convective flow.

The variation of the temperature distribution in the radial direction of the slurry droplet with drying time is described by the following equation

$$\frac{\partial}{\partial t}\left(\rho_d C_{p,d} T_d\right) = \frac{1}{r^2}\frac{\partial}{\partial r}\left(k_d r^2 \frac{\partial T_d}{\partial r}\right) \quad (1)$$

where r is the radial position in the droplet, t is the drying time, $T_d, \rho_d, C_{p,d}$ and k_d are the temperature, density, heat capacity and heat conductivity of the slurry droplet, respectively.

The temperature profile is symmetrical with respect to the droplet centre and the corresponding boundary condition is

$$\frac{\partial T_d}{\partial r} = 0 \text{ at } r = 0 \quad (2)$$

The boundary condition at the droplet surface is

$$h(T_g - T_d) = k_d \frac{\partial T_d}{\partial r} - \lambda_w \rho_{d,w} \frac{dR_d}{dt} \text{ at } r = R_d(t) \quad (3)$$

where R_d is the droplet radius, T_g is the temperature of drying gas, h is the heat transfer coefficient and α_w is the latent heat of water evaporation. In derivation of Eq. (3), the temperature of drying gas is assumed to be constant. The heat supplied to the outer surface of the droplet by drying gas is transferred toward the droplet centre by conduction and also consumed for water evaporation from the droplet surface. The position of this boundary varies in time as the slurry droplet shrinks.

The droplet shrinkage rate is proportional to the evaporation rate dm/dt as

$$\frac{dR_d}{dt} = -\frac{1}{\rho_{d,w} S_d}\frac{dm_v}{dt} \quad (4)$$

where S_d is the droplet surface area.

The initial condition for Eq. (4) is

$$R_d = R_{init} \quad \text{at } t = 0 \quad (5)$$

where R_{init} is the initial droplet radius.

The evaporation rate equation is

$$\frac{dm_v}{dt} = k_m S_d (\rho_{v,s} - \rho_{v,b}), \quad (6)$$

where k_m is the mass transfer coefficient, $\rho_{v,s}$ and $\rho_{v,b}$ are the densities of water vapor at the droplet surface and in the bulk air, correspondingly.

Assuming water vapor as an ideal gas, the densities of water vapor are

$$\rho_{v,s} = \frac{M_w p_{v,s}(T_d)}{R_{gas} T_d}, \quad \rho_{v,b} = \frac{M_w p_{v,b}(T_g)}{R_{gas} T_g} \quad (7)$$

where M_w is the molecular weight of water vapor, R_{gas} is the universal gas constant, $\rho_{v,s}$ and $\rho_{v,b}$ are the vapor pressures the droplet surface and in the bulk air, respectively.

The slurry droplet density is calculated presuming an ideal two-component mixture as

$$\rho_d = \frac{(1+X)\rho_{d,s}\rho_{d,w}}{\rho_{d,w} + X\rho_{d,s}} \quad (8)$$

where X is the moisture content of the slurry droplet defined as the amount of water relative to the solid amount in a droplet :

$$X = \frac{m_{d,w}}{m_{d,s}} = \frac{m_d(1+X_{d,0})}{m_{d,0}} \quad (9)$$

where m_d is the current droplet weight and $m_{d,0}$ is the droplet initial weight.

The thermal conductivity of slurry droplet is calculated using a series resistance model (Chen et al., 2005) as

$$k_d = \varepsilon_d k_w + (1-\varepsilon_d)k_s \quad (10)$$

where k_w and k_s are the thermal conductivities of water and solids, respectively, and ε_d is the droplet voidage.

Similarly, the specific heat of slurry droplet for the ideal mixture is (Kirillin et al., 1956)

$$C_{p,d} = \frac{XC_{p,w}}{1+X} + \frac{C_{p,s}}{1+X} \quad (11)$$

where $C_{p,w}$ and $C_{p,s}$ are the heat capacities of water and solids, respectively.

The following empirical correlations are used to evaluate the heat and mass transfer coefficients (Ranz et al., 1952)

$$Nu = \frac{h \cdot 2R_d}{k_g} = 2 + 0.65\left(\frac{2R_d V_g \rho_g}{\mu_g}\right)^{0.5}\left(\frac{C_{p,g}}{\mu_g k_g}\right)^{0.33} \quad (12)$$

$$Sh = \frac{k_m \cdot 2R_d}{D_{wv}} = 2 + 0.65\left(\frac{2R_d V_g \rho_g}{\mu_g}\right)^{0.5}\left(\frac{\mu_g}{\rho_g D_{wv}}\right)^{0.33} \quad (13)$$

where Nu and Sh are the Nusselt and Sherwood numbers for drying gas, correspondingly. Here, V_g is the velocity of drying gas, D_{wv} is the diffusivity of water vapor, k_g, μ_g, ρ_g *and* $C_{p,g}$ are the thermal conductivity, viscosity, density and heat capacity of drying gas, respectively. During the first phase of drying, the heat and mass coefficients increase with time according to Eqs. (12) and (13) due to the droplet shrinkage.

The diffusivity of water vapor is given as (Grigoriev et al., 1988)

$$D_{wv} = 3.564 \cdot 10^{-10}\left(T_d + T_g\right)^{1.75} \quad (14)$$

Second phase of drying

The particle composed of a dry porous crust and a wet core is formed at the end of first phase of drying. During the second drying phase, the receding evaporation boundary is assumed to exist that separates the dry crust layer from the wet core [9], as shown in figure 1.

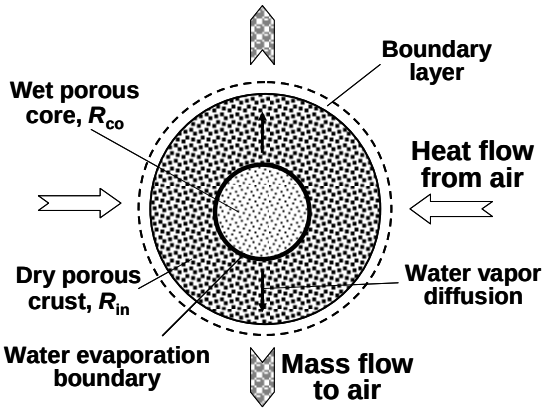

Fig 1: Model of drying a slurry droplet

Water vapor formed at the evaporation boundary diffuses first through the porous crust and then in the atmosphere surrounding the droplet. The outside radius of the crust shell, R_{in}, remains constant throughout this period, but the wet porous core diminishes as the evaporation progress. The temperature distribution in the radial direction of the wet core is calculated by solving the following heat balance equation

$$\frac{\partial}{\partial t}\left(\rho_{co} C_{p,co} T_{co}\right) = \frac{1}{r^2}\frac{\partial}{\partial r}\left(k_{co} r^2 \frac{\partial T_{co}}{\partial r}\right) \quad (15)$$

where $T_{c0}, \rho_{c0}, C_{p,c0}$ *and* k_{c0} are the temperature, density, heat capacity and heat conductivity of the wet core, respectively.

The boundary condition at the particle centre is

$$\frac{\partial T_{co}}{\partial r} = 0 \text{ at } r = 0 \quad (16)$$

The heat balance on the outer surface of the wet core yields

$$\lambda_w \rho_{d,w} \varepsilon \frac{dR_{co}}{dt} = k_{co} \frac{\partial T_{co}}{\partial r} - k_{cr} \frac{\partial T_{cr}}{\partial r} \text{ at } r = R_{co}(t) \quad (17)$$

where k_{cr} is the heat conductivity of the crust layer.

The energy conservation equation for the crust region is

$$(1-\varepsilon)\rho_s C_{p,s} \frac{\partial T_{cr}}{\partial t} = \frac{k_{cr}}{r^2} \frac{\partial}{\partial r}\left(r^2 \frac{\partial T_{cr}}{\partial r}\right) + \frac{D_{cr} M_w C_{p,wv}}{r^2} \frac{\partial}{\partial r}\left(r^2 T_{cr} \frac{\partial C_{wv}}{\partial r}\right) \quad (18)$$

where ε is the voidage of the crust layer and D_{cr} is the diffusivity of water vapor in the pore space of the crust layer.

The boundary condition at the particle outer surface is (Dalmaz et. al, 2007)

$$-k_{cr} \frac{\partial T_{cr}}{\partial r} = h\left(T_{cr} - T_g\right) \text{ at } r = R_{in} \quad (19)$$

and the corresponding boundary condition at the inner surface of the crust layer, i.e. the outer surface of the wet core, is

$$T_{co} = T_{cr} \text{ at } r = R_{co}(t) \quad (20)$$

The concentration of water vapor at various radial positions in the crust layer is calculated by solving the mass balance equation

$$\varepsilon \frac{\partial C_{wv}}{\partial t} = D_{cr} \left[\frac{\partial C_{wv}^2}{\partial r^2} + \frac{2}{r} \frac{\partial C_{wv}}{\partial r} \right] \quad (21)$$

The corresponding boundary conditions for Eq. (21) are

$$-D_{cr} \frac{\partial C_{wv}}{\partial r} = k_m \left(C_{wv} - C_g\right) \text{ at } r = R_{in} \quad (22)$$

$$C_{wv} = \frac{p_v(T_{cr})}{R_{gas} T_{cr}} \text{ at } r = R_{co}(t) \quad (23)$$

The receding rate of crust-wet core interface is obtained from the mass balance at the evaporation interface as

$$\varepsilon \rho_w \frac{dR_{co}}{dt} = D_{cr} M_w \frac{dC_{wv}}{dr} \quad (24)$$

The initial condition for Eq. (24) is

$$R_{co} = R_{in} \text{ at } t = 0 \quad (25)$$

The effective diffusion coefficient, D_{cr}, is evaluated by using the following correlation (Ochoa-Tapia et al., 1994)

$$D_{cr} = \frac{2\varepsilon D_{wv}}{3-\varepsilon} \quad (26)$$

RESULTS AND DISCUSSION

The spray drying of the slurry droplet containing colloidal silica particles (Nesic et al, 1991) was simulated using the developed model. The model partial and ordinary differential equations were solved using a difference method suitable for the moving boundary problems (Crank, 1984).

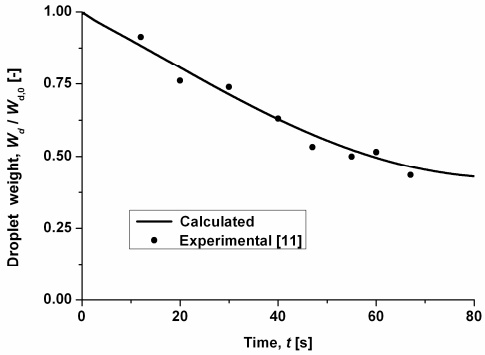

Fig 2: Comparison of calculated results with experimental data for drying of slurry droplet of silica particles

Comparison of calculated results and experimental data (Nesic et al, 1991) is shown in Figure 2 for drying air temperature of 101°C. The variation of the droplet weight with drying time was simulated separately for two drying phases and then combined in one curve in figure 2. The calculated curve is in a good agreement with experimental data points confirming the applicability of developed model.

Figure 3 illustrates the decrease of the droplet weight and the variation of the average droplet temperature with time during drying the slurry droplet having an initial radius of 1 mm. The drying gas temperature was set at 130°C.

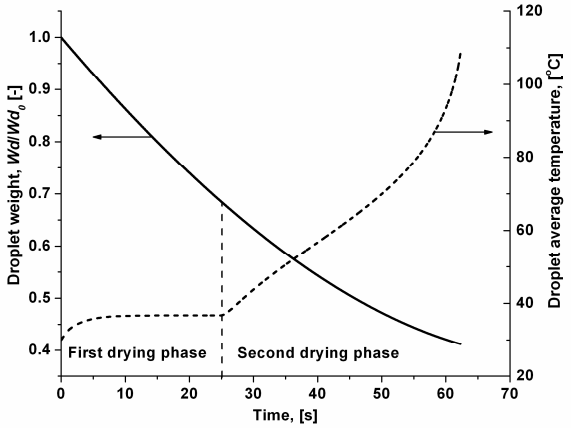

Fig 3: Variation of droplet weight and average droplet temperature during drying

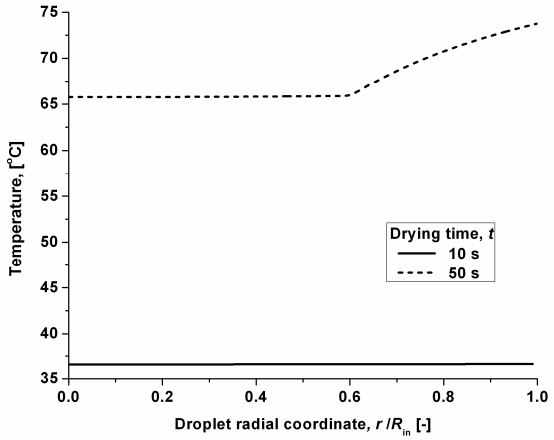

Fig 4: Temperature distributions in the slurry droplet

During the first drying phase, the weight of the droplet is calculated as

$$W_d(t)=\frac{4}{3}\pi\left(\rho_w\left(R_d^3(t)-R_{in}^3\right)+\rho_w\varepsilon R_{in}^3+\rho_s(1-\varepsilon)R_{in}^3\right) \quad (27)$$

and the droplet average temperature is evaluated using the temperature distribution in the droplet radial direction as

$$T_{av}=\frac{3}{R_d^3(t)}\int_0^{R_d(t)} r^2T(r)dr \quad (28)$$

The droplet weight and the droplet average temperature at the second drying phase are calculated from the following equations

$$W_d(t)=\frac{4}{3}\pi\left(\rho_w\varepsilon R_{co}^3(t)+\rho_s(1-\varepsilon)R_{in}^3\right) \quad (29)$$

$$T_{av}=\frac{3}{R_{in}^3}\int_0^{R_{in}} r^2T(r)dr \quad (30)$$

During the first drying phase, after the short heating-up period, the average temperature remains constant as all the heat transferred from the air is consumed for evaporation of water from the droplet surface. At the second phase, the average temperature increases until it approaches the temperature of the surrounding gas, as illustrated in figure 3.

Figure 4 shows the temperature distributions within the droplet at drying time of 10 and 50 s. The temperature distribution is almost uniform during the first drying phase for *t* = 10 s. The temperature distribution in the second stage, t = 50 s, is sharp in the crust region and uniform in the wet core region. The temperature difference between the droplet surface and the wet core increases with drying time due to growth of the layer of dry crust which represents the resistance to the heat transfer.

Figures 5 and 6 illustrate the effect of the drying gas temperature on the droplet weight loss and the crust build up, respectively. The evaporation rate of the slurry droplet significantly increases at high drying gas temperature resulting in a thicker crust layer and lighter droplets for the same drying time.

Figures 7 and 8 illustrate the effect of the initial droplet size on the droplet weight loss and the thickness of the crust layer, respectively. The shorter drying time is required for the smaller droplet due to the enhanced evaporation rate as a result of the high mass and heat transfer rates. The mass and heat transfer coefficients calculated by

Eqs. (12) and (13) are summarized in Table 1 for droplets of 100 and 1000 μm in radius.

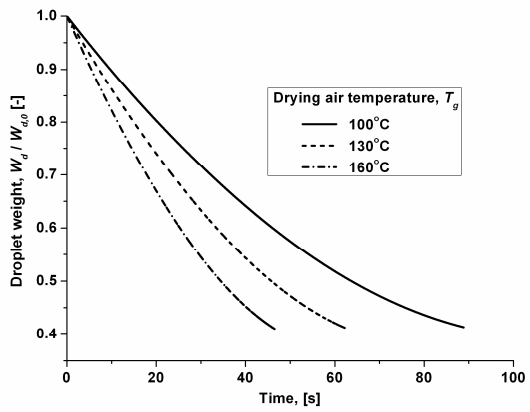

Fig 5: Effect of drying gas temperature on droplet weight loss

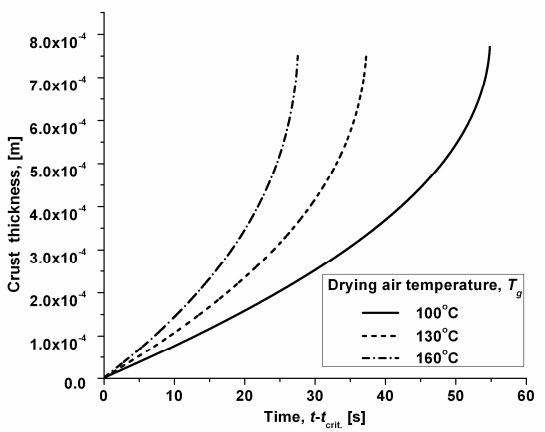

Fig 6: Effect of drying gas temperature on thickness of dry crust layer.

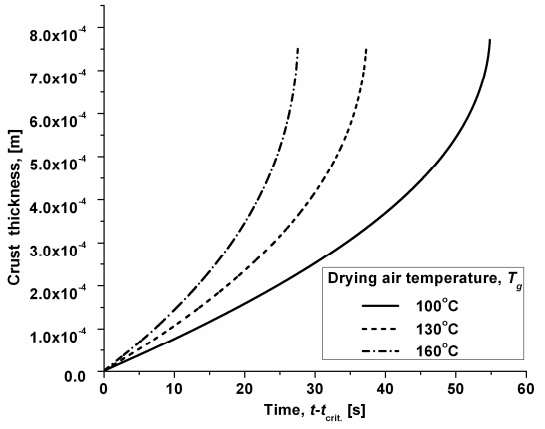

Fig 7: Effect of initial droplet size on droplet weight loss

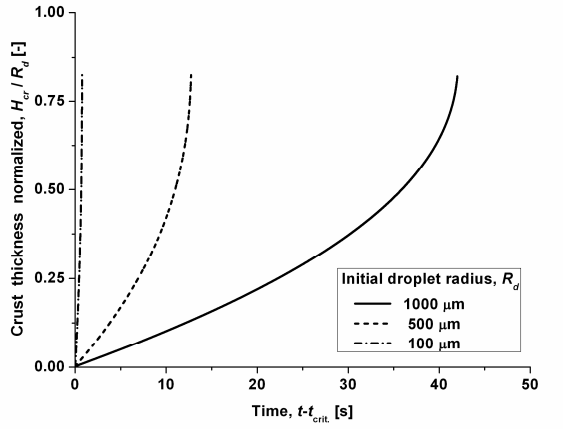

Fig 8: Effect of initial droplet size on thickness of dry crust layer.

Table 1 . Variation of mass and heat transfer coefficients during drying.

Initial droplet radius, R_d [μm]	Mass and heat transfer coefficients	
	Drying phase	
	Beginning	End
100	k_m [m/s] = 0.737	0.835
	h [W/m^{2}K] = 662.2	742.9
1000	k_m [m/s] = 0.157	0.195
	h [W/m^{2}K] = 142.8	160.5

CONCLUSION

The detail model was developed for the description of the drying kinetics of slurry droplet by considering simultaneous heat and mass transfer processes during spray drying. The temperature and moisture distributions within the slurry droplet were calculated for the first and second drying phases. The parametric study revealed that the droplet drying time decreases with increasing the drying gas temperature and decreasing the droplet diameter.

The devised model could be incorporated into the overall model of spray dryer to optimize the operational parameters or to design new processes.

REFERENCES

1) Chen, X.D., Peng, X.F. (2005). "Modified Biot number in the context of air drying of small moist porous objects," *Drying Technology*, *23*, 83-103.
2) Crank, J. (1984). "*Free and moving boundary problems*," Oxford.
3) Elek, N., Hoffman, R., Raviv, U., Resh, R., Ishaaya, I., Magdassi, S. (2010). "Novaluron nanoparticles: Formation and potential use in controlling agricultural insect pests," *Colloids Surf. A*, *372*, 66-72.
4) Dalmaz, N., Dzbelge H.O., Erasalan A.N., Uludag Y. (2007). "Heat and Mass Transfer mechanisms in drying of a suspension droplet : a new computational model," *Drying Technology*, 25, 391 – 400.
5) Farid, M. (2003). "A new approach to modelling of single droplet drying," *Chem. Eng. Sci.*, *58*, 2985-2993.
6) Gharsallaoui, A., Roudauta, G., Chambina, O., Voilleya, A., Saurela, R. (2007). "Applications of spray-drying in microencapsulation of food ingredients: An overview," *Food Research International*, *40*, 1107-1121.
7) Grigoriev, V.A., Zorin, V.M. (1988). "*Thermal engineering handbook*," Energoatomizdat, Moscow.
8) Kirillin, V.A., Sheindlin, A.E. (1956). "*Thermodynamics of solutions*," Energy, Moscow.
9) Masters, K. (1985). "*Spray Drying Handbook*," Longman Scientific and Technical.
10) Mezhericher, M., Levy, A., Borde, I. (2010). "Theoretical models of single droplet drying kinetics: a review," *Drying Technology*, *28,* 278-293.
11) Nesic, S., Vodnik, J. (1991). "Kinetics of droplet evaporation," *Chem. Eng. Sci.*, *46*, 527-537.
12) Ochoa-Tapia, J.A., Stroeve, P., Whitaker, S. (1994). "Diffusive transport in two-phase media: spatially periodic models and Maxwell's theory for isotropic and anisotropic systems," *Chem. Eng. Sci.*, *49*, 709-726.
13) Okuyama, K., Abdullah, M., Lenggor, I.W., Iskandar, F. (2006). "Preparation of functional nanostructured particles by spray drying," *Advanced Powder Technology*, *17*, 587-611.
14) Ranz, W.E., Marshall, W.R. (1952). "Evaporation from drops," *Chem. Eng. Prog.*, *48*, 141-146, 173-180.
15) Soottitantawat, A., Bigeard, F., Yoshii, H., Furuta, T., Ohgawara, M., Linko, P. (2005). "Influence of emulsion and powder size on the stability of encapsulated D-limonene by spray drying," *Innovative Food Science and Emerging Technologies*, *6*, 107-114.